SHORT SCIENTIFIC COMMUNICATION

Numerical simulations of block-and-ash flows using the Titan2D flow model: examples from the 2006 eruption of Merapi Volcano, Java, Indonesia

S. J. Charbonnier · R. Gertisser

Abstract We present Titan2D simulations of two well-characterized block-and-ash flow (BAF) events of the 2006 eruption of Merapi (Java, Indonesia) that affected the Gendol valley on the volcano's southern flank and adjacent, densely populated interfluve (non-valley) areas: (1) a single dome-collapse event to the south that generated one of the smaller, post-June 14 flows and (2) a sustained, multiple dome-collapse event, also directed to the south, that produced the largest flows of the 2006 eruption emplaced in the afternoon of June 14. Using spatially varying bed friction angles, Titan2D is capable of reproducing the paths, velocities, runout distance, areas covered and deposited volumes of these flows over highly complex topography. The model results provide the basis for estimating the areas and levels of hazards associated with BAFs generated during relatively short as well as prolonged dome-collapse periods and guidance during future eruptive crises at Merapi.

Keywords Numerical modelling · Titan2D · Block-and-ash flow · Hazard assessment · Merapi

Introduction

Block-and-ash flows (BAFs), generated by gravitational or explosive collapse of viscous lava domes, are common at many subduction-related volcanoes where they pose a permanent threat to life, property and infrastructure. BAFs triggered by gravitational dome collapse are nowhere as frequent as at Merapi, an andesitic volcanic complex in heavily populated Central Java, Indonesia (Fig. 1). About sixteen of Merapi's past eruptions have caused fatalities and, during the latest eruptive episode in 2006, BAFs affected areas outside the main river channels previously considered relatively safe from such flows. This has highlighted the unpredictable and poorly understood behaviour of Merapi's flows and the urgent need for improved and reliable geophysical mass flow models to better assess the potential hazard of such flows. Despite the fact that BAFs are amongst the most dangerous volcanic phenomena, only a small number of realistic numerical simulations of actual events over accurate 3-D terrain, using various computational models, have been published (e.g., Wadge et al. 1998; Itoh et al. 2000; Pitman et al. 2003; Sheridan et al. 2004; Bursik et al. 2005; Saucedo et al. 2005; Rupp et al. 2006; Macías et al. 2008; Widiwijayanti et al. 2008). The aims of this paper are to apply the Titan2D flow model (Patra et al. 2005) to simulate well-characterized BAFs from the 2006 eruption of Merapi (Charbonnier and Gertisser 2008) and to define key flow parameters that will allow more reliable predictions of the areas and levels of hazards associated with BAFs during future eruptions at Merapi.

The 2006 eruption of Merapi

After five years, volcanic activity at Merapi resumed with the extrusion of a new lava dome in March 2006. Lava-dome growth increased during April and was rapidly followed by periods of multiple rockfalls and dome-collapse pyroclastic flows during May and early June

S. J. Charbonnier (✉) · R. Gertisser
School of Physical and Geographical Sciences,
Earth Sciences and Geography, Keele University,
Keele,
Staffordshire ST5 5BG, UK
e-mail: s.charbonnier@epsam.keele.ac.uk
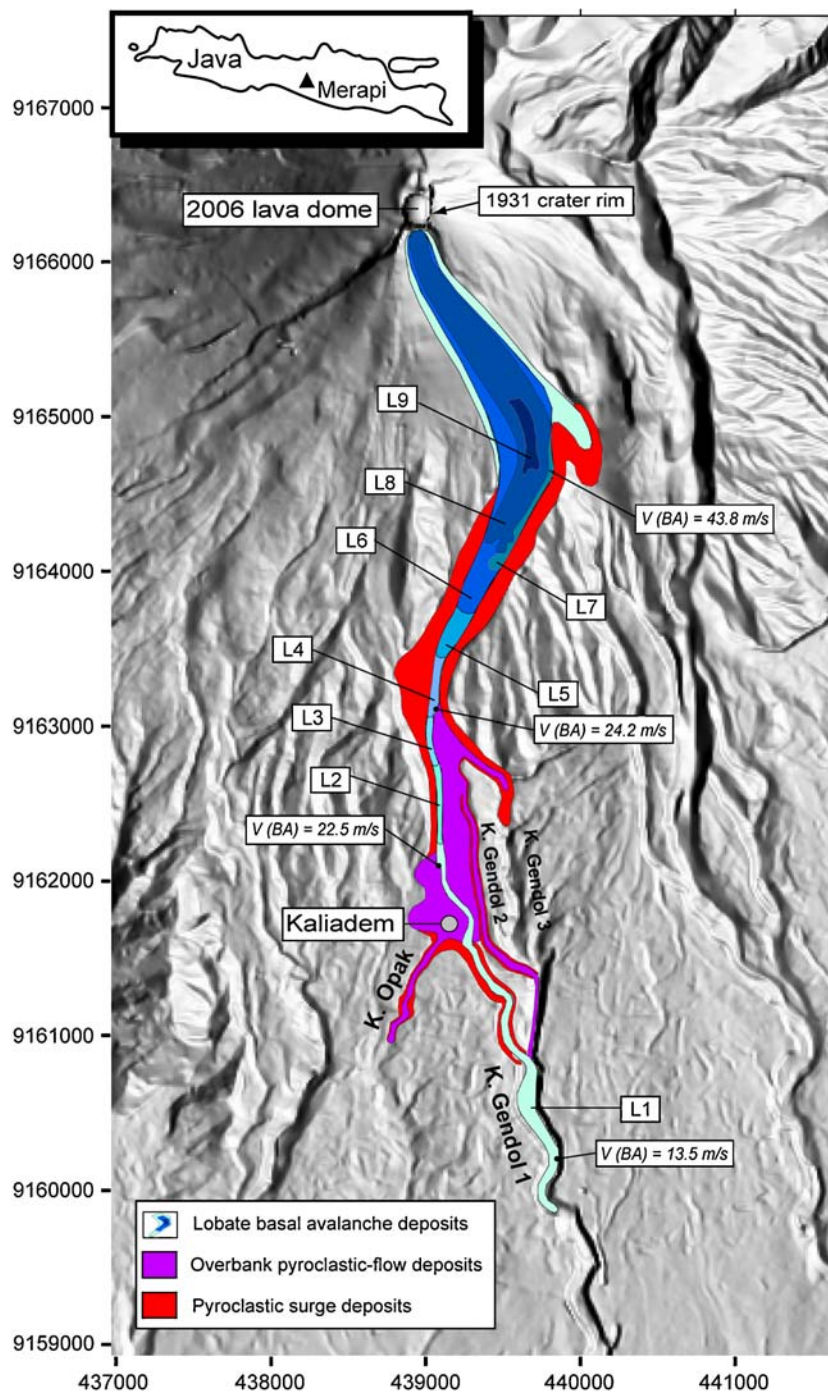
Fig. 1 Map of the June 2006 block-and-ash flow deposits on the southern flank of Merapi (after Charbonnier and Gertisser 2008) superimposed on a digital elevation model. Individual lobe numbers (L1-L9) and minimum velocity calculations at flow bends for the basal avalanche (V (BA)) of the June 14 afternoon flow (lobe 1) are also shown. Coordinates are in UTM meters. The inset map shows the location of Merapi volcano in Central Java

2006 that were directed toward the south-western and southern flanks of the volcano. Following partial collapse of the south-eastern part of the 1931 crater wall at the beginning of June 2006 (Fig. 1), which had functioned as a barrier to prevent pyroclastic flows travelling southward, the activity peaked on June 14 with two sustained dome-collapse events. These lasted over periods of tens of minutes to produce two major BAFs with runout distances in the Gendol valley of 5 and 7 km, respectively (Charbonnier and Gertisser 2008). The largest of these flows caused two fatalities and destruction in the village of Kaliadem, ~4.5 km from Merapi (Fig. 1). After June 14, the

number and frequency of BAFs decreased until the end of the eruption in early July.

The valley-filling basal avalanche deposits of the June 2006 flows form nine overlapping lobes in the Gendol valley (Fig. 1), which were produced by successive flows generated during and after the major dome-collapse events on June 14. Associated overbank deposits cover adjacent interfluves and fill the surrounding valleys. Related ash-cloud surge deposits are found along valley margins. Inferred flow velocities for the basal avalanche, based on field studies of the June 14 BAFs (Charbonnier and Gertisser 2008), vary from 43.8 to 13.5 m/s (Fig. 1).

The BAFs generated during the peak of activity on June 14 are interpreted as long-runout, voluminous flows that swept broader sectors on Merapi's southern flank and were capable of escaping from channel confines to produce overbank deposits on either side of the Gendol valley. The volcano monitoring record (BGVN 2007) suggests that these flows were generated by sustained, multiple dome-collapse events over a period of approximately two hours. The BAFs generated after June 14 were short- to medium-runout granular flows that were generated by short, single collapses of parts of the 2006 lava dome (Charbonnier and Gertisser 2008).

Numerical simulations

The Titan2D model

The Titan2D computer program (Patra et al. 2005) is built on a depth-averaged model for an incompressible Coulomb continuum, a "shallow water" granular flow, based on the work of Savage and Hutter (1989), Iverson (1997), Iverson and Denlinger (2001), Denlinger and Iverson (2001) and Mageney-Castlenau et al. (2003). It combines numerical simulations of a flow with digital elevation data of natural terrain supported by a Geographical Information System (GIS) interface. The conservation equations for mass and momentum are solved with a Coulomb-type friction term for the interactions between the grains of the media and between the granular material and the basal surface (Pitman et al. 2003). The model assumes that the flow starts as an ellipsoidal pile of material with user-specified dimensions of height, width and thickness as well as the starting location coordinates. The two other input parameters are the internal friction angle and the basal or bed friction angle. The direct outputs are flow depth and momentum, which can be used to compute field observable variables at different locations and times during the flow, such as run-up height, inundation area, velocity and time of flow. The latest release of the Titan2D code allows the simulation of material that actively extrudes from the ground at a specific

rate over a specific period of time by using a combination of different piles and flux sources (i.e., multiple-collapse events).

Application to the 2006 block-and-ash flows of Merapi

We used Titan2D to simulate two well-characterized BAFs of the 2006 eruption of Merapi: (1) a single, discrete (45 s) collapse of a small portion ($\sim 1.0 \times 10^6 \, \mathrm{m}^3$) of the 2006 lava dome to the south where the material was shed as one pulse and generated one of the smaller, post-June 14 flows (lobe 5 in Fig. 1) and (2) a sustained, multiple dome-collapse event (five pulses over a period of 300 s), also directed to the south, where a significant portion ($\sim 6.0 \times 10^6 \, \mathrm{m}^3$) of the 2006 lava dome collapsed incrementally to produce the largest flows of the 2006 eruption emplaced in the afternoon of June 14 (lobe 1 in Fig. 1). The duration and number of collapse events for the two case studies are based on observational monitoring records (BGVN 2007) and seismic data of the pyroclastic activity during the eruption (J. Wassermann, pers. comm. 2007).

Previous authors have shown the importance of the digital elevation model (DEM) resolution on computational routines for reconstructing the different paths, velocities and extents of various flows, and for correctly estimating the areas and levels of hazards associated with future volcanic activity (e.g., Stevens et al. 2002; Pitman et al. 2003). In the present work, computational modelling was performed on a DEM of Merapi (courtesy of C. Gerstenecker, TU Darmstadt, Germany) with a spatial resolution of 15 m, a vertical accuracy of ±9 m and a post-1994 eruption topographic surface (C. Gerstenecker, pers. comm. 2009). In order to account for recent topographic changes, the upper slope topography was adjusted to fit the situation after the collapse of the south-eastern crater wall and before the peak activity on June 14, 2006 (Charbonnier and Gertisser 2008). The changes of the DEM included the creation of a collapse structure on the upper south-eastern slopes and the addition of a synthetic dome topography in the summit area to allow the generation of BAFs from the 2006 lava dome (Fig. 1). These adjustments were based on aerial and land-based photographs and field observations by the authors in 2006. In order to increase computational power, decrease computing time and allow for the use of such a large data set, the simulations were performed using the KHAOS supercomputer cluster available at Keele University.

Sheridan et al. (2005) showed that Titan2D simulations are not sensitive to internal friction angles, so a common value of 30° was taken for granular materials in line with values used by other authors (Pitman et al. 2003; Stinton et al. 2004; Bursik et al. 2005; Sheridan

et al. 2005; Rupp et al. 2006; Macías et al. 2008). The simulations are, however, highly sensitive to the bed friction and can be greatly improved by the incorporation of spatially varying bed friction angles, as single bed friction values for models over a complex topography, different surface materials and through varying channel slopes and morphologies can lead to several discrepancies with actual events (Stinton et al. 2004). Here, the use of variable bed friction values in our simulations has proven to be vital, as none of the simulations performed using a single bed friction was capable of reproducing the path and extent of the actual events. Based on a slope map generated from the DEM and an elevation profile along the June 2006 flow path (Charbonnier and Gertisser 2008), the construction of a GIS-based classified map, which matches the area covered by the DEM, was used to define zones in the region where pronounced changes in the topographic surface (i.e., slope breaks and channel confinements and morphologies) result in a change in the bed friction angle. During computation, Titan2D queries the classified map and bed friction angle list to find the appropriate friction value.

Based on the actual flow parameters (Charbonnier and Gertisser 2008), a series of evaluation criteria has been developed for the determination of best-fit bed friction values that form the basis for evaluating the validity of our models: (1) the runout distance of the simulated flows should match those of the lobe fronts as mapped in the field, (2) the distribution of the deposits and the deposited volume should fall within the range of those of the actual flows, (3) the velocities of the flows and deposit thicknesses should be comparable to those calculated and observed in the field and (4) the flow simulations of the multiple-collapse events must escape from channel confines to fill the interfluve area (in particular the area around Kaliadem) and to be re-channeled into the adjacent valleys (Fig. 1).
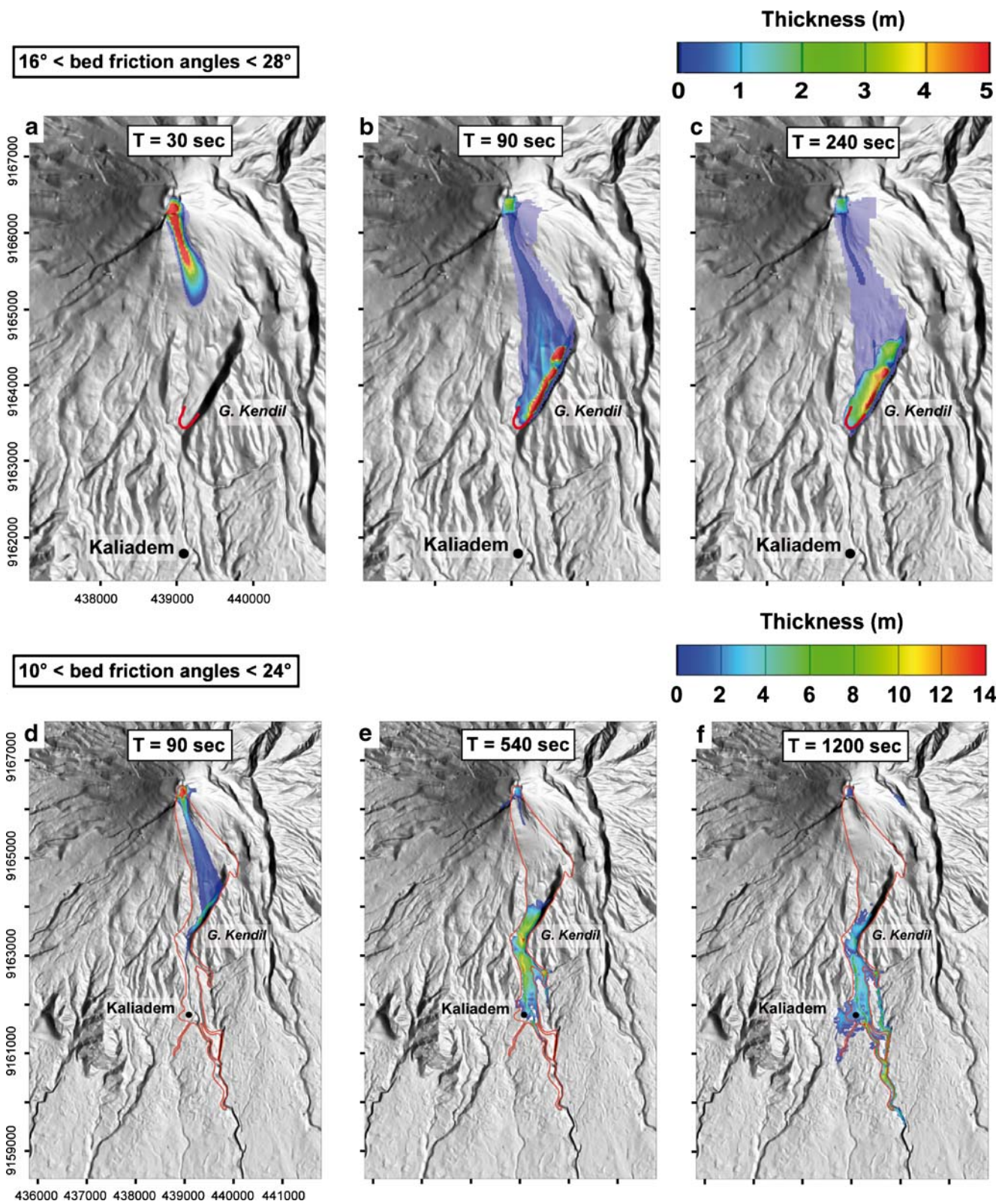
Results

The Titan2D modelling results for the two types of BAFs, including the best-fit spatially varying bed friction values used, are shown in Fig. 2. The average flow velocities and maximum thickness profiles are illustrated in Fig. 3. The average velocities are computed by considering the velocity of various computational cells, which range from 0 m/s to values significantly above the mean. It is noteworthy that these velocities do not correspond to those recorded at the flow front. However, they can be compared to the minimum velocities determined at flow run-up onto obstacles perpendicular to the flow direction and superelevation along the outside of bends in confined channels (Fig. 1).

Case study 1: Single dome-collapse event (Post-June 14, 2006 block-and-ash flow)

After descending the steepest slopes of the southern flank of the volcano, the simulated flow hits the western side of Gunung (Gunung means hill in Indonesian) Kendil, bends 45° (Fig. 2b) and stops after ~4 minutes (Fig. 2c). Results between the simulated and the actual event (lobe 5 in Fig. 1) are comparable in terms of runout distance (3.4 km), area covered (~0.4 km²) and deposited volume (~$0.9 \times 10^6 \, m^3$) (Charbonnier and Gertisser 2008). The velocity and thickness profiles predicted by the model (Fig. 3) show three successive flow stages. The simulated flow experienced both, a sudden decrease in velocity and an increase in thickness after 50 s, when the collapse at the source stops and the flow reaches the first break in slope with inclinations below 30° at 2.0 km from the summit. This rapid change of the flow behaviour corresponds to the transition from an accumulative to a depletive, non-uniform current (Kneller and Branney 1995). The final depositional stage begins when the thickness of the flow decreases after ~100 s and the velocity drops to a constant background value (Figs. 2b and 3). The simulated deposits are mainly distributed over an area between 2.0 and 3.4 km from the summit and below the first break in slope (Fig. 2c) in agreement with field observations of the lobe 5 deposits.

Case study 2: Multiple dome-collapse event (June 14, 2006 block-and-ash flow)

The simulated flow follows the topography of the southern flank and when upon reaching the base of G. Kendil, bends 45° and enters the medial area of Kali (Kali means river in Indonesian) Gendol. Here, the flow is first channeled into the main valley (K. Gendol 1) and then overspills its eastern margin, spreads laterally and fills the interfluves to produce overbank pyroclastic flows that enter K. Gendol 2 and K. Gendol 3 (Figs. 1, 2d and e). After 4 min, the flow overspills the western side of K. Gendol 1, reaches the village of Kaliadem located 4.5 km from the summit, and is then re-channeled into the Opak valley to the southwest. Having reached the distal parts of the Gendol valley, the main flow slows down considerably and travels the remaining 2.5 km over the course of the next 15 min. It completely stops after ~20 min with a maximum runout distance of 7.4 km (Fig. 2f). Results compare favourably with those obtained by field analyses of the June 14 afternoon flow deposits (lobe 1 in Fig. 1) in terms of runout distance (7 km for the actual event), area covered (1.51 and 1.85 km² for the simulated and actual deposits, respectively) and collapsed volume (~$6.0 \times 10^6 \, m^3$ in both cases). Moreover, the overall thickness distribution of the simulated deposits is in close agreement with measured thicknesses at

Fig. 2 Titan2D simulation results showing the thickness distribution within the flows during emplacement and the resulting final deposits. Coordinates are in UTM meters. (a—c) Single dome-collapse event. Red outline is the mapped extent of the lobe 5 front deposits. (d—f) Multiple dome-collapse event. Red outline is the mapped extent of the June 14 flow deposits
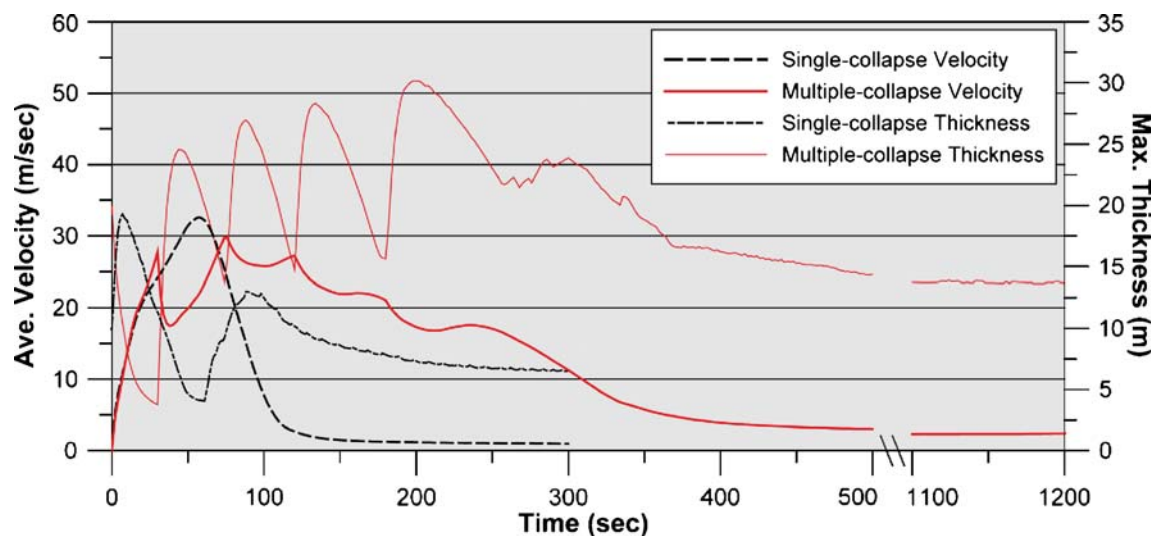
Fig. 3 Average velocity and maximum thickness profiles obtained during the simulation of the single and multiple dome-collapse events. See text for explanations

exposed cross sections of lobe 1 deposits, which vary from 4–20 m for the valley-filling deposits and from 2–8 m for the overbank deposits. The simulation is capable of reproducing some of the local features (run-up onto obstacles and superelevation along the outside of bends) that characterise the June 14 deposits and, to some extent, illustrates the ability of such flows to bank up, thicken and overspill the main channel margins to produce overbank pyroclastic flows. However, some discrepancies with field data are noted and the velocity and travel time of the flow are not reproduced entirely. Strong variations of maximum thickness and average velocity during the simulation (Fig. 3) are directly related to variations in the source conditions, resulting in five periods of decreasing velocities and increasing thicknesses in response to the generation of the five pulses at the source. Comparison of Titan2D average velocities with those calculated in the field at particular locations along the flow path (Fig. 1) leads to underestimations of ~30% in the proximal area to ~80% in the distal reaches. These underestimated flow velocities result in an unrealistic travel time of 20 min for the flow to reach the observed runout distance. The distribution of the simulated deposits differs slightly from the one mapped in the field with the complete filling of the easternmost river valley, K. Gendol 3, down to the junction with K. Gendol 2 (see Fig. 1 for locations), the widespread filling of the Kaliadem interfluve area to the west, beyond the extent of the actual deposits (Fig. 2f), and the lack of any proximal deposits in the area less than 2.5 km from the summit.

Implications for hazard assessment at Merapi

A sensitivity analysis of the multiple dome-collapse event was carried out by examining the role of varying bed

friction angles, pile dimensions and volume of the initial material, as described by Sheridan et al. (2005). For example, increasing the collapsed volume by 100% from 6 to $12 \times 10^6 \, \text{m}^3$ produces a flow with comparable runout distance and increases the area covered by 77% and the maximum deposit thickness by 17%. Decreasing all bed friction angles by 20% results in the generation of flows that overcome the resisting forces and remain mobile during extended computational time (>30 min). Increasing all bed friction values by 20% leads to a 21% decrease in runout length (from 7.4 to 5.8 km) and a further increase by 50% leads to a 37% decrease in runout length (from 7.4 to 4.7 km). These results suggest that the performance of the Titan2D flow model in simulating actual events is critically dependent on (1) the calibration of the model by using extensive field-based data such as deposit distribution, processes of flow generation, transport and deposition, (2) the incorporation of spatially varying basal frictions into the model and (3) the choice of input parameters, such as location and volume of the initial pile and source characteristics (single or multiple dome-collapse, dome-collapse duration and volume of collapsed material).

Titan2D modelling have allowed the reconstruction of the paths and extents of single and multiple dome-collapse events generated during the 2006 eruption of Merapi and a better characterization of the key parameters that control their flow behaviour, namely bed friction angles, volumes and discharge rate. We emphasize that the simulations are capable of reproducing the mobility of voluminous and successive BAFs closely spaced in time over a period of several minutes, like those of June 14, 2006 that overspilled the margins of the Gendol valley and flowed across the interfluve area around Kaliadem (Fig. 1). Due to their potential of being re-channeled into adjacent river valleys

and sometimes to flow laterally away from the main channel confines, these overbank pyroclastic flows are considered the most hazardous part of BAFs (Charbonnier and Gertisser 2008). The recent morphological changes of the summit area during the 2006 eruption and the unpredictable and poorly understood conditions that lead to the development of such overbank flows at Merapi now mean that areas previously considered safe (i.e. interfluve areas in the southern sector of the volcano) must be regarded under increased levels of risk from such flows. The delineation of these key areas at risk from overbank pyroclastic flows are currently not adequately represented in the actual hazard map (Purbawinata et al. 1996) where the three danger zones and associated scenarios are based on three general types of volcanic hazards (pyroclastic flows, surges and lahars). The model evaluation presented here provides the basis for estimating the areas and levels of hazards associated with BAFs generated by single and multiple dome-collapse periods and guidance for improving disaster mitigation plans at Merapi. Comparison of the Titan2D modelling results obtained in this study with numerical simulations performed using other computer routines, like the "VolcFlow" model developed at the Laboratoire Magmas et Volcans, Clermont-Ferrand, France (Kelfoun and Druitt 2005), will help to improve the assessment of the hazard and risk potential of such flows.

References

BGVN (2007) Smithsonian Institution, Washington, DC 32(2):3–8

Bursik M, Patra AK, Pitman EB, Nichita C, Macías JL, Saucedo R, Girina O (2005) Advances in studies of dense volcanic granular flows. Rep Prog Phys 68:271–301

Charbonnier SJ, Gertisser R (2008) Field observations and surface characteristics of pristine block-and-ash flow deposits from the 2006 eruption of Merapi Volcano, Java, Indonesia. J Volcanol Geotherm Res 177:971–982

Denlinger RP, Iverson RM (2001) Flow of variably fluidized granular material across three-dimensional terrain: 2. Numerical predictions and experimental tests. J Geophys Res 106:553–566

Itoh H, Takahama J, Takahashi M, Miyamoto K (2000) Hazard estimation of the possible pyroclastic flow disasters using numerical simulation related to the 1994 activity at Merapi Volcano. J Volcanol Geotherm Res 100:503–516

Iverson RM (1997) The physics of debris flows. Rev Geophys 35:245–296

Iverson RM, Denlinger RP (2001) Flow of variably fluidized granular material across three-dimensional terrain: 1. Coloumb mixture theory. J Geophys Res 106:537–552

Kelfoun K, Druitt TH (2005) Numerical modeling of the emplacement of Socompa rock avalanche, Chile. J Geophys Res 110:B12202

Kneller B, Branney MJ (1995) Sustained high-density turbidity currents and the deposition of thick massive sand. Sedimentology 42:607–616

Macías JL, Capra L, Arce JL, Espíndola JM, García-Palomo A, Sheridan MF (2008) Hazard map of El Chichón volcano, Chiapas, México: constraints posed by eruptive history and computer simulations. J Volcanol Geotherm Res 175:444–458

Mageney-Castlenau A, Vilotte JP, Bristeau MO, Perthame B, Bouchut F, Simeoni C, Yernemi S (2003) Numerical modelling of avalanches based on Saint Venant equations using a kinetic scheme. J Geophys Res 108:2527. doi:10.1029/2002JB002024

Patra AK, Bauer AC, Nichita CC, Pitman EB, Sheridan MF, Bursik MI, Rupp B, Webber A, Stinton AJ, Namikawa LM, Renschler CS (2005) Parallel adaptive simulation of dry avalanches over natural terrain. J Volcanol Geotherm Res 139:1–22

Pitman EB, Patra AK, Bauer A, Sheridan MF, Bursik MI (2003) Computing debris flows and landslides. Phys Fluids 15:3638–3646

Purbawinata MA, Ratdomopurbo A, Sinulingga IK, Sumarti S, Suharno I (1996) Merapi volcano–a guide book. Volcanological Survey of Indonesia, Bandung

Rupp B, Bursik MI, Namikawa L, Webb A, Patra AK, Saucedo R, Macías JL, Renschler CS (2006) Computational modeling of the 1991 block and ash flows at Colima Volcano, Mexico. In: Siebe et al. (eds) Neogene-Quaternary continental margin volcanism: A perspective from México. Geol Soc Am Spec Paper 402:237–252

Saucedo R, Macías JL, Sheridan MF, Bursik MI, Komorowski JC (2005) Modeling of pyroclastic flows of Colima Volcano, Mexico: implications for hazard assessment. J Volcanol Geotherm Res 139:103–115

Savage SB, Hutter K (1989) The motion of a finite mass of granular material down a rough incline. J Fluid Mech 199:177–215

Sheridan MF, Hubbard B, Carrasco-Nuñez G, Siebe C (2004) Pyroclastic flow hazard at Volcán Citlaltépetl. Nat Haz 33:209–221

Sheridan MF, Stinton AJ, Patra AK, Pitman EB, Bauer A, Nichita CC (2005) Evaluating Titan2D mass-flow model using the 1963 Little Tahoma Peak avalanches, Mount Rainier, Washington. J Volcanol Geotherm Res 139:89–102

Stevens NF, Manville V, Heron DW (2002) The sensitivity of a volcanic flow model to digital elevation model accuracy: experiments with digitized map contours and interferometric SAR at Ruapehu and Taranaki volcanoes, New Zealand. J Volcanol Geotherm Res 119:89–105

Stinton AJ, Sheridan MF, Patra AK, Dalbey K, Namikawa LM (2004) Integrating variable bed friction into Titan2D mass-flow model: application to the Little Tahoma Peak avalanches, Washington. Acta Vulcanol 16:153–163

Wadge G, Jackson P, Bower SM, Woods AW, Calder E (1998) Computer simulations of pyroclastic flows from dome collapse. Geophys Res Lett 25:3677–3680

Widiwijayanti C, Voight B, Hidayat D, Schilling SP (2008) Objective rapid delineation of areas at risk from block-and-ash pyroclastic flows and surges. Bull Volcanol. doi:10.1007/s00445-008-0254-6